Evidence for dislocations or related defects present in CdTe and $Cd_{1-x}Zn_xTe$ Crystals

Salah A. Awadalla[1], Alan W. Hunt[1], Russell. B. Tjossem[1], Kelvin G. Lynn[1], Csaba Szeles[2], Mary Bliss[3]
[1]Center for Materials Research, Washington State University, Pullman WA 99163; [2] eV PRODUCTS, II-VI Inc., Saxonburg, PA 16056; [3]Pacific Northwest National Laboratory, Richland, WA 99352

ABSTRACT

Thermoelectric Effect Spectroscopy and Thermally Stimulated Current measurements were used to investigate trapping levels in semi-insulating CdTe and $Cd_{1-x}Zn_xTe$ crystals from multiple ingots grown by vertical Bridgman with over pressure control and high-pressure Bridgman methods. The crystals from different growth methods have different dislocation densities as well as Zn concentrations. The thermal ionization energies of these levels were extracted using both the variable heating rate and initial rise methods; the trapping cross sections were then calculated using the temperature maximum method. We report here that the shallow levels observed at E_1=0.11±0.02 and E_2=0.17±0.02 eV are intrinsic and the latter level is most likely related to the dislocation density.

Keywords: Intrinsic defects, Dislocation, CdTe, $Cd_{1-x}Zn_xTe$, TEES.

1. INTRODUCTION

CdTe and $Cd_{1-x}Zn_xTe$ semi-insulating compounds are promising materials for room temperature, x-ray, and γ ray radiation detector applications[1]. This potential originates from their high atomic number, which provides good absorption for high-energy radiation, and their large band gap, which minimizes promotion of charge carriers from the valence band to the conduction band resulting in lower thermal noise. However, the advancement of these semiconductor compounds as commercial radiation detectors has been impeded by carrier trapping at localized defect levels within the band gap, which results in incomplete charge collection and therefore poor detector performace[2]. The characterization and understanding of the electrical properties of these localized defect levels is imperative to detector improvement.

The effect of the dislocation generated during crystal growth on the electrical properties of CdTe and $Cd_{1-x}Zn_xTe$ has not been thoroughly investigated. The goal of this paper is to show that the shallow levels present in "high purity" semi-insulating CdTe and $Cd_{1-x}Zn_xTe$ crystals grown by Vertical Bridgman with Over Pressure control (VBOP) and High Pressure Bridgman (HPB) methods are intrinsic and related to dislocations or related defects. The crystals from different growth methods have different dislocation densities as well as Zinc concentrations. The difference in dislocation densities has two sources. The first source is the difference in the growth technique and the temperature gradient during growth. It has been reported that HPB grown crystals have more dislocations as compared to crystals grown by the VBOP method because of the typically steeper temperature gradients used[3]. The second source is the difference in Zinc concentrations. It is reported that the higher the ionicity (CdTe has ionicity of 0.71) the smaller the formation energy of dislocations and stacking faults. With an increasing incorporation of the Zn, the CdTe lattice exhibits higher shear modulus resulting in a lower density of both dislocations and sub-grains[4]. We have focused our investigation on two major defect levels observed at approximately 0.11eV and 0.17 eV.

2. METHODOLGY

2.1 I-V Measurements

The current-voltage (I-V) measurements are used to extract the resistivity of the samples and check the contact's ohmicity. I-V measurements are done at room temperature using a Keithley 6105 resistivity adapter and Keithley 273 source meter. The samples were measured in two different bias ranges (±1V, and ±100V). The resistivities of the samples were calculated from a range of different voltages using the following formula [5]:

$$\rho = \frac{R \cdot A}{L} \tag{1a}$$

Where *R* and *A* are the resistance and contact area of the sample and L is thickness. The contact's ohmicity, b, is extracted from:

$$|I| = a \cdot |V|^{b} \tag{1b}$$

Where I is the current, V is the voltage, and a is material constant. The contact is ohmic when b ≅ 1.

2.2 Thermoelectric Effect Spectroscopy (TEES) Measurement

In this technique thermal excitation is used to release charge carriers from the localized levels within the band gap to the valence or conduction band. The charge carriers are swept out of the sample by applying a temperature gradient (TEES)[6,7] across the sample. TEES mainly offers three advantages. First, TEES extends the sensitivity of the experiment to higher temperatures where deeper levels can be detected. Second, in principle TEES distinguishes between electron and hole traps. Third, TEES determines whether the sample is n or p-type. In this technique, the sample is placed on a sapphire stage and is held stationary with spring-loaded plunger within a closed-cycle cryostat. After placing the sample in the cryostat, the system is pumped to approximately a pressure of 10^{-6} torr; the sample was then cooled to about 10 K in the absence of light. At about 10 K the sample is illuminated with 1.33 eV photons from an infrared light diode (935 nm), until the photo-excitation current saturates. The diode is then turned off and the sample is heated at a constant rate up to 350 K causing a gradual emptying of the localized levels by thermal excitation. The temperature at which a trap empties is related to its thermal ionization energy. The thermal ionization energy of the localized levels is calculated by both the variable heating rate and the initial rise methods.

2.2.2 Variable Heating Rate

In this method the traps are emptied at different heating rates while all other parameters are kept constant. The equation relating the heating rate to the temperature maximum of the current peak is given by [8]

$$\ln\left(\frac{T_{\max}^{2}}{\beta}\right) = \frac{E_{th}}{k_b \cdot T_{\max}} - \ln\left(\frac{w \cdot k_b}{E_{th}}\right) \qquad \text{with} \qquad w = N_c \cdot \sigma \cdot V_{th} \tag{2}$$

where T_{max} is the temperature of the current peak maximum, β is the heating rate, k_b is Boltzmann's constant, E_{th} is the thermal energy of the trap, w is the escape attempt frequency, N_c is the effective density of states in the conduction band, σ is the trapping cross section area, and V_{th} is the thermal velocity.

As the heating rate increases from one measurement to another, the centroid of the current peak associated with a trap shifts to higher temperatures. Using different heating rates, β_1, β_2, β_3, one gets different temperature maximums, T_1, T_2, T_3 respectively. Plotting $\ln(T_{\max}^{2}/\beta)$ versus $1/k_bT_{max}$ results in a straight line with a slope equal to the trap's thermal energy, E_{th}. Also it is important to consider the possibility of retrapping in which the freed charge carriers undergo retrapping by empty deep levels. This effect will lead to an increase of the magnitude of the measured deep trap current peak relative to the shallow trap's current peak, which in turns leads to a change of the concentration of trapped charge.

2.2.3 Initial Rise Method

This method relates to the thermal ionization energy according to the following equation [8]

$$I(T) = A \cdot Exp\left(\frac{E_{th}}{k_b \cdot T}\right) \tag{3}$$

Hence plotting ln (I) versus of $1/k_bT$ produces a straight line at the initial rise of the peak. The slope of this line is equal the thermal ionization of the trap, E_{th}.

The extracted thermal energy values from the above methods with corresponding maximum temperatures are used to calculate the trapping cross section according to the following equation [9].

$$\sigma = \frac{\beta \cdot E_{th}}{C \cdot m^* \cdot T_{\max}^4} \exp\left(\frac{E_{th}}{k_b \cdot T_{\max}}\right) \qquad \text{With} \qquad C = \left(\frac{4 \cdot k_b^3 \sqrt{6\pi^3}}{h^3}\right) \tag{4}$$

Where m^* is the effective mass of the charge carrier. In CdTe $m^* = 0.14 * m_0$ for electrons and $m^* = 0.37 * m_0$ for holes, with m_0 being the charge rest mass and h is Planck's constant.

3. Data and Samples Information

Three samples were investigated in this paper. Two of them were grown by HPB at eV PRODUCTS and the third was grown by VBOP at Honeywell Inc. The two HPB samples are CdTe and $Cd_{0.8}Zn_{0.2}Te$ and the VBOP is $Cd_{0.966}Zn_{0.034}Te$. The purity data of the samples and the Zn concentration are shown below in table 1.

Element (ppb) / Sample	C	N	O	Na	Mg	Si	Al	Cl	Ni	Fe	Cu	P	Ga	Zn*
HPB CdTe (eV)	54	36	180	3	18	4	13	2	2	15	2	ND	ND	0%
HPB $Cd_{0.8}Zn_{0.2}Te$ (eV)	26	17	76	ND	78	2	18	ND	ND	ND	ND	2	2	20%
VBOP $Cd_{0.966}Zn_{0.034}Te$ (Honeywell)	1700	100	930	ND	ND	ND	5	ND	ND	ND	ND	ND	ND	3.4%

Table 1: Impurity concentrations in the samples studied measured by glow discharge mass spectroscopy (GDMS).
1ppb = $3 * 10^{13}$ cm $^{-3}$ ND= Not Detected
Other shallow and deep levels forming elements such as Li, F, In, V, Ti, Co, and Cr are below the detection limit of the GDMS
*Zn concentration is reported as x value through out the paper

The samples were etched in 5% Br-methanol and Br-ethanol for 2.5 and 1.5 minutes respectively, rinsed with methanol, and then Au contacts were sputter deposited. Etch pit density studies were done by the suppliers on CdTe grown by HPB and CdZnTe grown by VBOP. The extracted dislocation densities for the samples are $10^6/cm^2$ and $10^5/cm^2$ respectively.

4. RESULTS AND DISCUSSION

4.1 I-V Measurements

The measured current-voltage (I-V) curves are shown in figure 1. Starting from these curves the resistivity and the contact's ohmicity are determined and shown in Table 2.

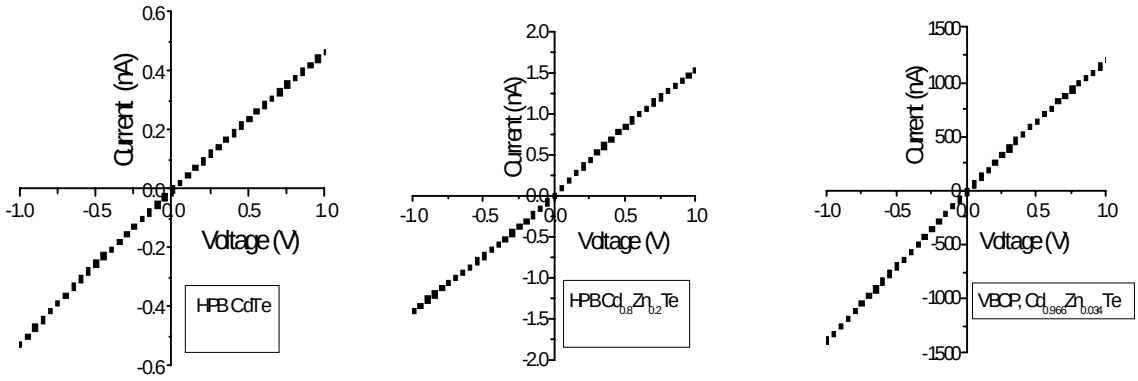

Figure 1: I-V curves of studied samples

Sample	Resistivity Ωcm	Ohmicity coefficient b	Sample type
HPB CdTe (eV)	(1.57± 0.04) x10^9	b(+) = 0.97±0.01 b(-) = 1.02±0.01	p
HPB $Cd_{0.8}Zn_{0.2}Te$ (eV)	(1.28± 0.02) x10^9	b(+) = 0.88±0.01 b(-) = 0.95±0.01	n
VBOP $Cd_{0.966}Zn_{0.034}Te$ (Honeywell)	(6.44± 0.24) x10^5	b(+) = 0.92±0.01 b(-) = 0.99±0.01	p

Table 2: Calculated resistivity and ohmicity of the studied samples

The resistivity is calculated from a number of voltage ranges to ensure that contact effects do not affect the calculated bulk resistivity of the samples. I-V measurements at ±100 V showed a significant leakage current for all three samples; therefore, no detector performance measurements were done. Also, from the calculated coefficient of ohmicity a slight asymmetry of the contact is observed. The origin of this asymmetry is undetermined; however, it could possibly due to the different level of surface irregularity or passivation. The signs (+) and (-) next to the b coefficient represent the polarity of the bias voltage.

From the calculated resistivity, one can see that HPB samples are "high resistivity" semi-insulating. Such a high resistivity samples are obtained by sufficiently controlling the Cd vacancy concentration during the growth, which can be accomplished by applying a high-pressure inert gas as in HPB or by using Cd over pressure and post growth annealing in Cd vapors as in VBOP[9]. Secondly, the residual Cd vacancies can be eliminated by a compensation mechanism and at these low impurity concentrations the deep levels control the resistivity of the material.[10]

4.2 TEES Measurements

TEES spectra from the samples are shown in Figure 2. The induced current from the emitted charge is plotted as a function of sample temperature. The TEES spectra show evidence for several shallow peaks in the range of 40 to 120 K, including the two shallow peaks, ~65 and ~100 K on which our study focused. The thermal ionization energies of these two shallow peaks were calculated directly from the above-mentioned two methods. The calculated energies as well as the trapping cross sections are shown in table 2.

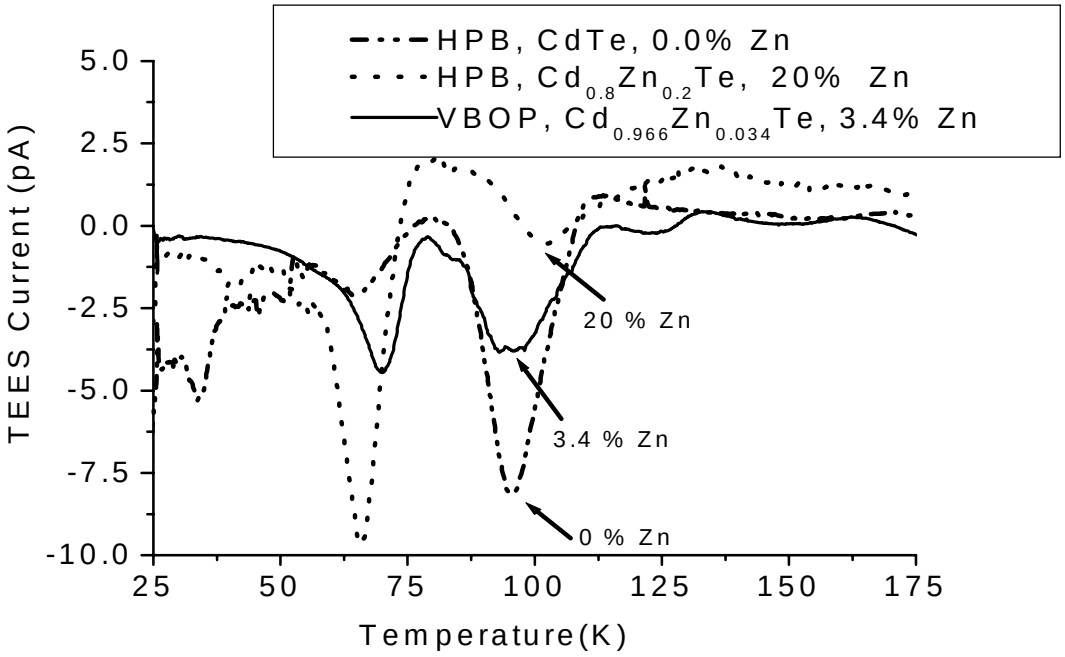

Figure 2: TEES spectra of the studied samples.

Sample	Peak Temp (K)	Energy from Variable heating rate (VHR) E_{th} (eV)	Trapping cross section Calculation from Variable heating Rate (VHR) σ (cm^2)	Energy calculation from Initial rise (IR) E_{th} (eV)	Trapping cross section calculation from IR σ (cm^2)	Average trapping cross section σ (cm^2)
HPB CdTe	64±1	0.14±0.02	$(8.6 \pm 32.6) \times 10^{-15}$	0.11±0.01	$(2.9 \pm 16.7) \times 10^{-17}$	$(5.8 \pm 24.6) \times 10^{-16}$
0% Zn	96±1	0.19±0.01	$(2.1 \pm 2.7) \times 10^{-16}$	0.15±0.02	$(1.3 \pm 3.3) \times 10^{-18}$	$(1.7 \pm 3.0) \times 10^{-17}$
VBOP $Cd_{0.966}Zn_{0.03}Te$	70±1	0.12±0.01	$(2.1 \pm 3.8) \times 10^{-17}$	0.1 ±0.01	$(6.4 \pm 11.4) \times 10^{-19}$	$(4.2 \pm 7.6) \times 10^{-18}$
3.4% Zn	96±1	0.165±0.02	$(8.7 \pm 22.1) \times 10^{-18}$	0.16±0.02	$(8.7 \pm 22.1) \times 10^{-18}$	$(8.7 \pm 22.1) \times 10^{-18}$
HPB $Cd_{0.8}Zn_{0.2}Te$	66±1	0.11±0.01	$(1.4 \pm 2.7) \times 10^{-17}$	0.1±0.01	$(3.4 \pm 6.5) \times 10^{-19}$	$(2.8 \pm 4.6) \times 10^{-18}$
20% Zn	101±1	0.19±0.01	$(3.0 \pm 3.6) \times 10^{-17}$	0.19±0.02	$(5.4 \pm 6.6) \times 10^{-17}$	$(4.2 \pm 5.1) \times 10^{-17}$

Table 3: Calculated thermal ionization energies and trapping cross sections for the levels at 65 K and 100 K in the studied samples

As is seen from the above table the calculated energy values for the $Cd_{1-x}Zn_xTe$ crystals from both methods are within the experimental error except for the HPB CdTe sample. The discrepancy in this sample partially arises from magnitude of overlapping peaks interfering with the level under study.

Because of the large magnitude of the error in the calculated trapping cross sections, we verified the values of the by the analysis of the photocurrent decay curves. This is done as follows: a sample was illuminated with 1.33 eV photons from an infrared diode under zero bias voltage at different constant temperature below the peak maximum until the photocurrent saturates. Then the diode is turned off and the decay of photocurrent as a function of time is fitted to extract the trap decay

time, τ_d, (i.e. the characteristic time of the thermally activated detrapping) for each temperature. The trap decay rate, $1/\tau_d$, is related to the trapping cross section and energy by the following expressions[8]

$$1/\tau_d = N_c \cdot \sigma \cdot V_{th} \cdot \exp\left(\frac{E_{th}}{k_b T}\right) \quad (5a)$$

or

$$\ln(1/\tau_d) = -\frac{E_{th}}{k_b T} + \ln(N_c \cdot \sigma \cdot V_{th}) \quad (5b)$$

where $N_c = 1.44 * 10^{14} * T^{3/2}$ cm $^{-3}$ and $V_{th} = 2.18 * 10^6 * T^{1/2}$ cm/s.

Plotting ln $(1/\tau_d)$ versus $1/k_bT$ results in a straight line with a slope equal to the trap thermal energy, E_{th}, and the intercept equal to ln $(Nc* \sigma * V_{th})$ from where the trapping cross section can be estimated. Note that in this calculation the weaker temperature dependence of N_c and V_{th} is neglected. The calculated trapping cross section for the first and the second peaks are $5.65*10^{-16}$ and $2.65*10^{-17}$ cm^2 respectively. This is in reasonable agreement with the values obtained from the TEES measurements. Figure 3 shows an example of the fitting to extract decay time, slope, and intercept from which the trapping cross sections are calculated.

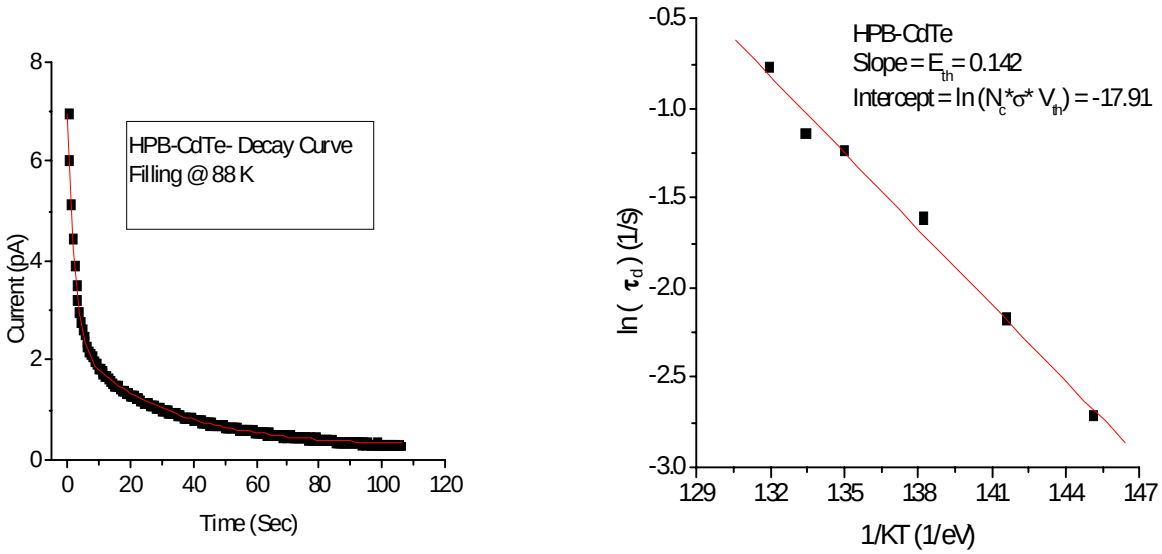

a) **b)**

Figure 3: a) Photocurrent decay for HPB CdTe measured at 88 K. b) Arrhenius plot of the trap decay time (τ_d) at various temperatures

The TEES spectra of sample HPB $Cd_{0.8}Zn_{0.2}Te$ are used as an example in order to demonstrate the energy calculations for both the variable-heating rates and initial rise methods. Figures 4a, and 4b show multiple TEES spectra with different heating rates, from 0.213 to 0.379 K/s, and plots of $\ln(T_{max}^2 / \beta)$ versus $1/k_bT_{max}$ for the extracted thermal energies for both peaks at 65 and 100 K respectively. Figure 5a and 5b show the TEES spectrum with inverted polarity and plots ln (I) versus $1/k_bT$ showing the thermal energy extraction using the initial rise method.

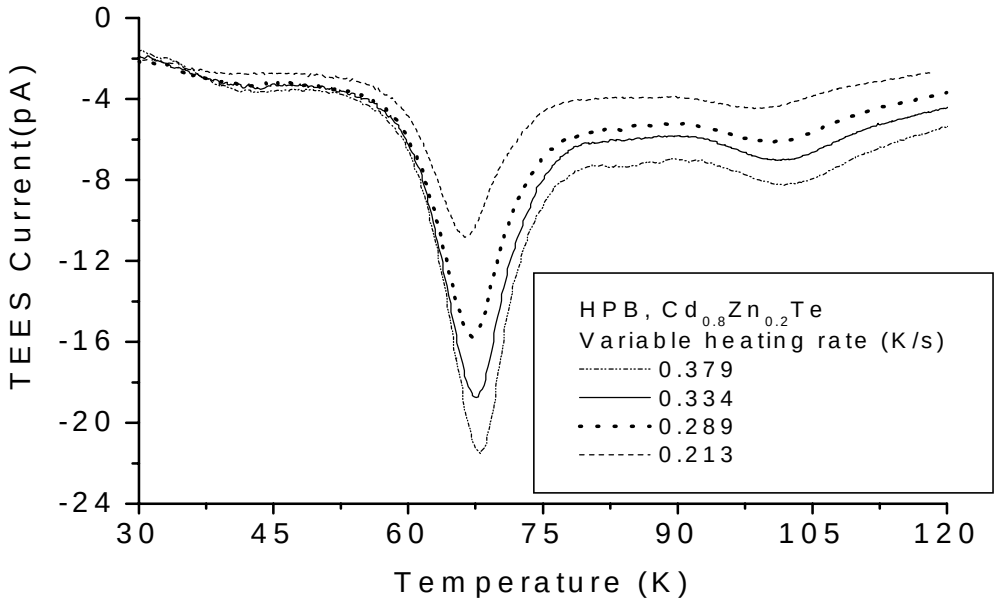

Figure 4a: TEES spectra with various heating rates ranging from 0.213 to 0.379 K/s.

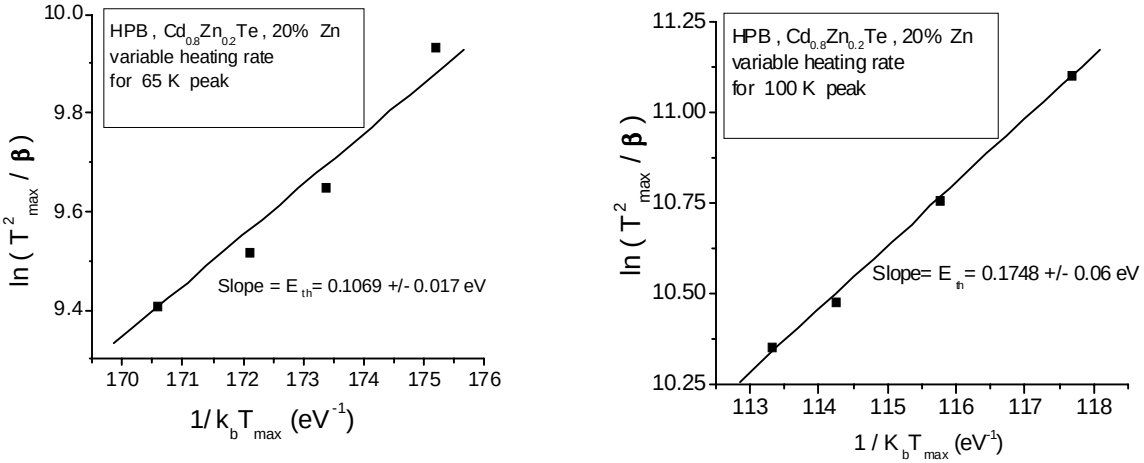

Figure 4b: Plots of ln (T_{max}^2 / β) versus $1/k_bT_{max}$ for the thermal energy extraction using variable heating rate method for the peaks around 65 K and 100K respectively.

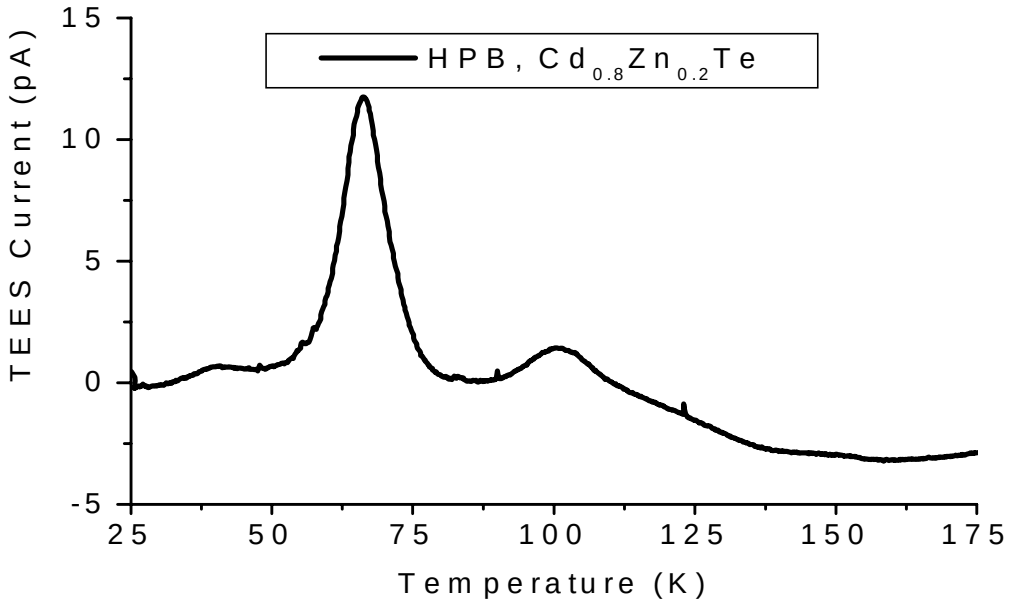

Figure 5a: TEES spectrum with inverted polarity used to determine the thermal energy using initial rise method

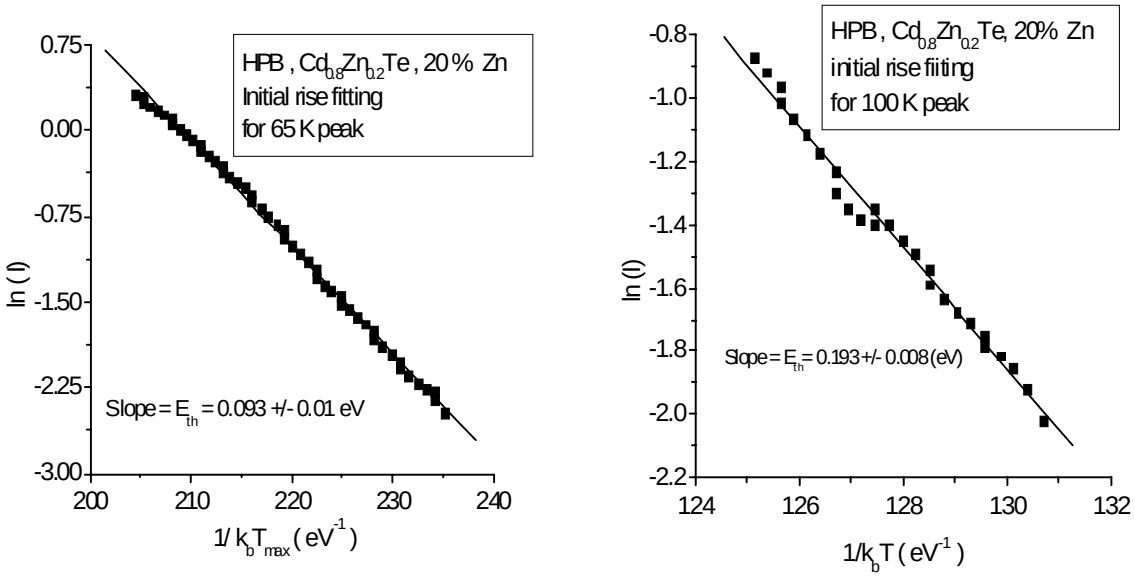

Figure 5b: Plot of ln (I) versus $1/k_bT$ for the thermal energy extraction using initial rise method for the peaks around 65 K and 100K respectively.

From table 1, elements with known shallow levels such as F and In are below the detection limit of the glow discharge mass spectroscopy (GDMS). Shallow level forming elements (i.e. Al) that are detected by GDMS are not present in sufficient quantities to explain the magnitude of the signals in the TEES spectra. In addition, no donor's peak is observed in the TEES spectra to justify the existence of any donor's level. This lack of shallow-level impurities implies that the levels at 0.11 and 0.17 (eV) are intrinsic. While it may be tempting to associate the level at 0.11 eV with A-centers, this is already ruled out by the purity data.

We propose that the second levels in question could most likely be attributed to dislocations or related defects.

Finally a number of points should be made about the relevance of these peaks to the radiation detector performance. First high concentrations of shallow levels lead to lower resistivity crystals, which in turn leads to higher noise levels. Secondly, it has been reported by P. Doty[11] that shallow level dislocations tend to organize into low energy configurations of mosaic of microstructure with dimensions of 100 micron, which directly and negatively affects electron transport within the crystal.

CONCLUSIONS

We have shown that the shallow levels in "high purity" semi-insulating CdTe and $Cd_{1-x}Zn_xTe$ crystals are intrinsic and related to dislocations or related defects, which have been confused with A-centers in other studies. The extract thermal ionization energies are 0.11±0.02 and 0.17±0.02 (eV) with trapping cross sections of $1.27 \pm 0.3 \times 10^{-16}$ and $2.51 \pm 0.4 \times 10^{-17}$ (cm^2) respectively assuming no retrapping which is most likely incorrect for dislocation. We have also correlated the second shallow level to the Zn concentration and it is effects on the dislocation density. Better control of these levels is required to produce high resistivity crystals.

ACKNOWLEDGEMENT

This work was supported by PNNL and NSF grants 240968AH7 and DMR9802712 respectively.

REFERENCES

[1] T.E. Schlesinger and R.B. James (eds.) "Semiconductors for room temperature Nuclear Detector Applications," (Academic, San Diego, 1995)

[2] A. Castadini, A. Cavallini, B. Fraboni, L. polenta, P. Fernandez, and J. Piqueras, "Cathodoluminescence and photoinduced current spectroscopy studies of defects in $Cd_{0.8}Zn_{0..2}Te$," *physical Review B*, **54**, 7622, 1996.

[3] C.J Johnson, E.E. Eisler, S.E. Cameron, Y. Kong, S. Fan, S. Jovanovic, and K.G. Lynn, "Crystallographic and metallurgical characterization of radiation detector grade CdTe materials," *Materials Research Society*, vol.302, p. 463-478, 1993.

[4] K. Guergouri, R. Triboulet, A. Tromsom-Carli, and Y. Marfaing, " Solution hardening and dislocation density reduction in CdTe crystals by Zn addition" *Journal of Crystal Growth*, **86**, 61-65, 1988.

[5] R. F. Pierret, *Semiconductor Device Fundamentals*, p.58-87, 483, and 587, Addison-Wesley Publishing company, Inc., New York, 1996.

[6] B. Santic, and U.V Desnica, "Thermoelectric effects spectroscopy of deep levels-Application to semi-insulating GaAs," *Applied physical letters*, **56**, 2636-2638, 1990.

[7] Z.C. Huang, K. Xie, and C.R. Wie, "A simple and reliable method of thermoelectric effect spectroscopy for semi-insulating II-VI semiconductors," *Rev. Sci. instrum.*, **62**, 1951-1954, 1991.

[8] R.H. bube, *Photoelectronic Properties of Semiconductors* , p. 149-188, Cambridge Press, Cambridge,1992.

[9] N. Krsmanovic, K.G. Lynn, M.H. Weber, R. Tjossem, Th. Gessmann, Cs. Szeles, E.E. Eissler, J.P. Flint, and H.E. Glass " Electrical compensation in CdTe and $Cd_{0.9}Zn_{0.1}Te$ by intrinsic defects," *Physical Review B*, Vol. **62**, 279-282, 2000.

[10] G. F. Neumark, "effect of deep levels on semiconductor carrier concentrations in the case of strong compensation," *Physical Review B*, vol. **26**, 2250-2252, 1982.

[11] F. P. Doty, Sandia National Laboratories, Unpublished progress report.